Journal of Alloys and Compounds 562 (2013) 111–115

Contents lists available at SciVerse ScienceDirect

Journal of Alloys and Compounds

journal homepage: www.elsevier.com/locate/jalcom

Ferromagnetic resonance properties of $Fe_{81-x}Ni_xGa_{19}$/Si(100) and $Fe_{81-y}Ni_yGa_{19}$/glass films

Chi-Ching Liu [a,b,*], Shien-Uang Jen [a], Jenh-Yih Juang [b], Chi-Kuen Lo [c]

[a] Institute of Physics, Academia Sinica, Taipei, Taiwan, ROC
[b] Dept. of Electrophysics, National Chiao Tung Univ., Hsinchu, Taiwan, ROC
[c] Dept. of Physics, National Taiwan Normal Univ., Taipei, Taiwan, ROC

ARTICLE INFO

Article history:
Received 23 November 2012
Received in revised form 25 January 2013
Accepted 25 January 2013
Available online 11 February 2013

Keywords:
FeNiGa films
Ferromagnetic resonance
Magnetostriction

ABSTRACT

Two series of $Fe_{81-x}Ni_xGa_{19}$/Si(100) and $Fe_{81-y}Ni_yGa_{19}$/glass films, where x or y = 0–26, were made by the magnetron sputtering method. The film thickness (t_f) was fixed at 100 nm. We have performed three kinds of experiments on these films: (i) the saturation magnetostriction (λ_S) measurement; (ii) the easy-axis and hard-axis magnetic hysteresis loop measurements; and (iii) the ferromagnetic resonance (FMR) experiment to find the resonance field (H_R) with an X-band cavity tuned at f_R = 9.6 GHz. The natural resonance frequency, f_{FMR}, of the Kittel mode at zero external field (H = 0) is defined as $f_{FMR} \fallingdotseq \nu[H_K 4\pi M_S]^{1/2}$, where $\gamma = 2\pi\nu$ is the gyromagnetic ratio, H_K and $4\pi M_S$ are the uniaxial anisotropy field and saturation magnetization, and $H_K << 4\pi M_S$. The Gilbert damping constant, α, is calculated from the formula, $\alpha = [\nu(\Delta H)_S]/(2f_R)$, where $(\Delta H)_{exp} = (\Delta H)_S + (\Delta H)_A$, $(\Delta H)_{exp}$ is the half-width of the absorption peak around the resonance field H_R, $(\Delta H)_S$ is the symmetric part of $(\Delta H)_{exp}$, and $(\Delta H)_A$ is the asymmetric part. The degree of asymmetry, $(\Delta H)_A/(\Delta H)_{exp}$, is associated with the structural and/or magnetic inhomogeneities in the film. The main findings of this study are as follows: (A) f_{FMR} tends to decrease, as x or y increases; (B) α decreases from 0.052 to 0.020 and then increases from 0.020 to 0.050, as x increases, and α decreases from 0.060 to 0.013 in general, as y increases; and (C) λ_S reaches a local maximum when x = 22. We conclude that the $Fe_{59}Ni_{22}Ga_{19}$/glass film should be the most suitable for application in magneto-electric microwave devices.

1. Introduction

The desirable properties of a soft magnetic material are high permeability (μ) and low loss. Hysteresis loss is the most important loss in ferromagnetic substances at low driving frequency. However, at the high driving frequency hysteresis loss becomes less important, because the domain-wall-displacement mechanism, is mostly damped and is replaced by the rotation-magnetization mechanism. Thus, the next important loss in ferromagnetic metals and alloys is the eddy current (EC) loss. Since a power loss of this type increases in proportion to the square of the frequency, it plays an important role at high frequencies, usually in the range of radio frequencies [1,2]. Moreover, if the frequency is increased further into the microwave range, one will encounter both the ferromagnetic resonance (FMR) and the EC phenomena.

In this study, we wish to find soft magnetic materials that can be used in a tunable magneto-electric microwave device [3] or other rf/microwave magnetic devices. In these devices, the basic requirements for the soft ferromagnetic film are low coercivity (H_C), high saturation magnetization ($4\pi M_S$), high saturation magnetostriction (λ_S), high rotational permeability (μ_r), high limiting (or natural resonance) frequency (f_{FMR}), high electrical resistivity (ρ), and low Gilbert damping parameter (α).

From Ref. [3], we find that the Fe–Ga alloys seem to be good soft magnetic materials for the device applications mentioned above. For example, they may have low saturation field (H_S), about 100 Oe for single crystals (SCs) and about 50 Oe for poly-crystals (PCs) [4,5], high saturation magnetization, about 18 kG [4], and high saturation magnetostriction, about 200–400 ppm for SC and about 40–100 ppm for PC sample [6,7]. Notice that although the FeGa single crystal has a large value of λ_S, which is favorable in terms of magneto-electric coupling, its ferromagnetic resonance line-width (ΔH), about 450–600 Oe [8] at X-band, is, however, too large for tuning efficiency. In other words, α of an FeGa single-crystal film is too large. Moreover, from an economic point of view, it is usually more laborious (or expensive) to grow a single-crystal than a poly-crystal film. Hence, in this paper we shall concentrate only on the polycrystalline film. Besides, it has been found that incorporation of about 12 at.% of a metalloid element, such as boron (B) or carbon (C), into the $Fe_{81}Ga_{19}$ alloy improves

* Corresponding author at: Institute of Physics, Academia Sinica, Taipei, Taiwan, ROC. Tel.: +886 2 27898909.
E-mail address: cloudboy1982@hotmail.com (C.-C. Liu).

0925-8388/$ - see front matter © 2013 Elsevier B.V. All rights reserved.
http://dx.doi.org/10.1016/j.jallcom.2013.01.169

λ_S; i.e., λ_S reaches maximum in the B range from 1 to 10 at.% [3,9–11]. Notice, however, there is a discrepancy between $\lambda_S \approx 70$ ppm for the $(FeGa)_{90}B_{10}$ film in Ref. [3] and $\lambda_S \approx 45$ ppm for the as-quenched $(FeGa)_{90}B_{10}$ bulk in Ref. [9].

In this study, we chose one series of the $Fe_{81-x}Ni_xGa_{19}$/Si(100) and another series of the $Fe_{81-y}Ni_yGa_{19}$/glass films, where x or y ranges from 0 to 26. Hopefully, we can achieve combinations of the following favorable features, such as low H_C or H_S, high $4\pi M_S$, high λ_S, high μ_r, high ρ, and low ΔH or α, from one of these FeNiGa films [12–14].

2. Experimental details

$Fe_{81-x}Ni_xGa_{19}$/Si(100) and $Fe_{81-y}Ni_yGa_{19}$/glass films, with $0 \leqq x$ or $y \leqq 26$ at.% Ni, were made by the magnetron sputtering method. The various fabrication conditions are summarized below: the base pressure (p) was 5×10^{-7} Torr; the Ar working gas pressure (p_{Ar}) was 5 m Torr; the sputtering power (P_w) was 80 W; the deposition temperature (T_S) was room temperature (RT); and the film thickness (t_f) was fixed at 100 nm.

The field-in-plane magnetic hysteresis loops was obtained from vibrating sample magnetometer (VSM) measurements. When the squareness ratio (SQR $\equiv M_r/M_S$) is the largest, we define the easy-axis (EA), and when SQR the smallest, the hard-axis (HA). In most cases, the angular dependence of SQR is roughly sinusoidal with a period of 180°. As an example, the HA hysteresis loop of the $Fe_{55}Ni_{26}Ga_{19}$/glass film in Fig. 1a shows that $(SQR)_{HA} = 0.72$, $H_S = 20$ Oe, and the anisotropy field ($H_K \equiv (1/2)(H_{K1} + H_{K2}) \approx 6.3$ Oe). For the same film, its EA hysteresis loop in Fig. 1b shows that the saturation magnetization ($4\pi M_S \approx 15.8$ KG), $(SQR)_{EA} = 0.99$, and coercivity ($H_C \approx 13.8$ Oe). Here, it is interesting to note that since $H_K \leqq H_C$ for all the films, they may be classified as the "inverted" films [15]. A brief summary is listed below: as x or y increases from 0 to 26, $4\pi M_S$ remains almost constant, 16.8–15.8 KG, and H_C decreases, 34.4–13.8 Oe.

The series of $Fe_{81-x}Ni_xGa_{19}$/Si(100) and $Fe_{81-y}Ni_yGa_{19}$/glass films, in a circular or disk shape, were studied with the FMR experiments. The microwave resonant cavity used was a Bruker ER41025ST X-band resonator, which was tuned at $f_R = 9.6$ GHz. The film samples were oriented such that EA//H and EA⊥h_{rf}, where H was an in-plane external field, which varied from 0 to 2 KOe, and h_{rf} was the microwave field. A typical FMR absorption spectrum of the $Fe_{70}Ni_{11}Ga_{19}$/glass film is shown in Fig. 2, where we can spot an FMR event or an absorption peak at $H = H_R$ and define the half-peak width $(\Delta H)_{exp}$. In this case, $H_R = 637$ Oe and $(\Delta H)_{exp} = 144$ Oe.

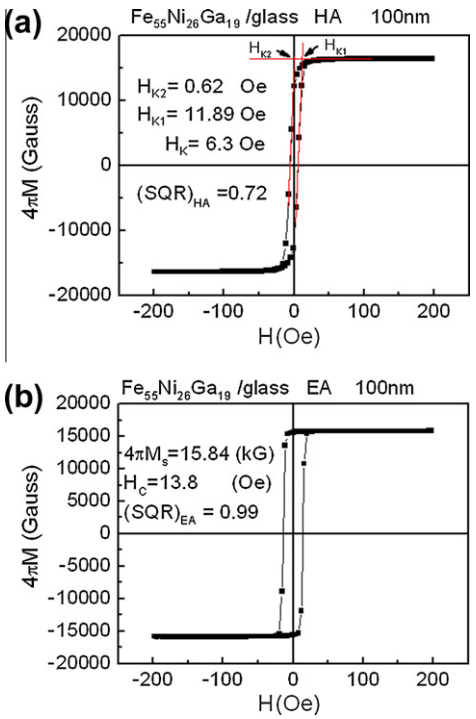

Fig. 1. (a) The hard-axis (HA) and (b) the easy-axis (EA) magnetic hysteresis loop of the $Fe_{55}Ni_{26}Ga_{19}$ film deposited on a glass substrate. H_K is the anisotropy field, $4\pi M_S$ is the saturation magnetization, H_C is the coercivity, and $(SQR)_{HA}$ and $(SQR)_{EA}$ are the squareness ratio along HA and EA, respectively.

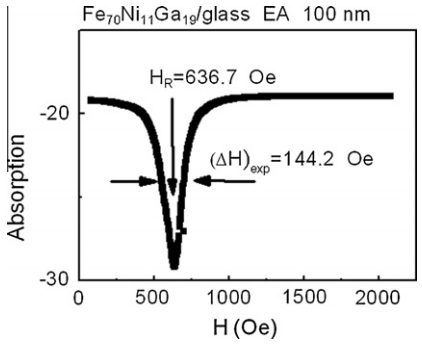

Fig. 2. A typical FMR absorption spectrum of the $Fe_{70}Ni_{11}Ga_{19}$/glass film at the microwave frequency $f_R = 9.6$ GHz.

The longitudinal and transverse magnetostrictions ($\lambda_{//}$ and $\lambda_\perp$) were measured in an optical-cantilever system [16]. The Young's modulus (E_f) of the each film, which is required in the estimations of $\lambda_{//}$ and $\lambda_\perp$, was obtained from nano-indentation measurements. Finally, λ_S was calculated using the formula $\lambda_S = (2/3)(\lambda_{//S} - \lambda_{\perp S}) = (2/3)\Delta\lambda$, where $\lambda_{//S}$ and $\lambda_{\perp S}$ are the $\lambda_{//}$ and $\lambda_\perp$ values above H_S.

The electrical resistivity (ρ) was measured by the standard four-point-probe method. The structural properties were characterized by X-ray diffraction (XRD) using Cu Kα_1 line.

3. Results and discussion

Table 1 lists the X-ray structure data of the $(FeNi)_{81}Ga_{19}$ films deposited on glass substrates. Briefly speaking, when $y = 22$ at.% Ni, there is only one single A2 phase, and when $y = 0$–17, and 26 at.% Ni, there are mixed phases with A2 (major) and $D0_{19}$, $L1_2$, and/or unidentified (minor) phases. In general, we consider that all the FeNiGa films are highly (110) textured.

Fig. 3 shows the main resonance field (H_R) at $f_R = 9.6$ GHz as a function of the Ni concentration (x or y) for the two series of $(FeNi)_{81}Ga_{19}$ films, respectively. From this figure, we find that H_R increases as x or y increases. When at the Kittle mode resonance, the relationship among H_R, H_K, f_R, and $4\pi M_S$ for a flat film can be written as [17–19],

$$(f_R/\nu)^2 = H_R^2 + (2H_K + 4\pi M_S)H_R + H_K(H_K + 4\pi M_S) \equiv X^2 \qquad (1)$$

where $\nu = \gamma/(2\pi$ is in MHz, $4\pi M_S$ and H's in Gauss, γ is the gyromagnetic ratio of the material and $g = \nu/(1.40X)$, with 1.40 in unit of MHz/G. From Eq. (1), we found that g of the FeNiGa films varies from 2.21 to 2.01, as x or y increases. Then, based on Eq. (1) and the g value, the natural (or FMR–K) resonance (at $H = 0$) would occur at $f_{FMR} = \nu[H_K(H_K + 4\pi M_S)]^{1/2} \fallingdotseq \nu[H_K 4\pi M_S]^{1/2}$ with $H_K << 4\pi M_S$. The plot of f_{FMR} vs. x or y is shown in Fig. 4. As discussed in the next paragraph, f_{FMR} should serve as the cut-off (or limiting) frequency (f_C) for these series of ferromagnetic films.

In general, the complex permeability, $\mu = \mu_R - i\mu_I$, has an anomalous behavior; the real part, μ_R, drops off and the imaginary part, μ_I, exhibits an absorption peak at a certain high frequency, e.g., f_C. For a non-metallic ferromagnet, f_C is mainly determined by FMR. For a metallic ferromagnet, according to Fig. 4.17 of Ref. [1], f_C should depend on the smallest dimension, i.e., t_f, of the sample. For example, if $t_f < \delta$, where $\delta = (\rho/\pi\mu_R f)^{1/2}$ is the skin depth, the μ_R or μ_I anomaly at f_C is related to the FMR effect, and if $t_f > \delta$, f_C is related to the eddy-current effect [1]. In our case, $t_f = 100$ nm $< \delta \approx 650$ nm (@$f \sim 1$ GHz). Thus, we would have $f_C = f_{FMR}$ for all the FeNiGa films in general. Here, since we do have metallic films, the eddy-current effect is not negligible, and should be considered in the resonance cases, as discussed later.

Table 1
Structural information: the X-ray diffraction peaks of the $Fe_{81-y}Ni_yGa_{19}$/glass films; I/I_{max} is the peak intensity ratio; and a is the lattice constant. $(\Delta H)_A/(\Delta H)_{exp}$ is the degree of asymmetry of the FMR linewidth. "?" means an unidentifiable diffraction peak.

y (at.% Ni)	2θ (deg.)	phase (hkl)	d (Å)	a (Å)	I/I_{max} (%)	$(\Delta H)_A/(\Delta H)_{exp}$ (%)
0	27.707	?	3.217	–	16.8	3.6
	38.300	$D0_{19}$(200)	2.348	–	14.5	
	44.570	A2(110)	2.031	2.873	100	
	82.421	A2(211)	1.169	–	10.6	
4	38.234	$D0_{19}$(200)	2.352	–	10.4	5.0
	44.537	A2(110)	2.033	2.875	100	
	82.124	A2(211)	1.173	–	5.6	
11	24.374	$L1_2$(100)	3.649	–	17.0	14.5
	29.456	?	3.030	–	87.9	
	44.570	A2(110)	2.031	2.873	100	
17	24.371	$L1_2$(100)	3.649	–	17.0	19.7
	44.570	A2(110)	2.031	2.873	100	
22	44.537	A2(110)	2.033	2.875	100	0.9
26	29.522	?	3.023	–	32.9	6.5
	44.669	A2(110)	2.027	2.867	100	

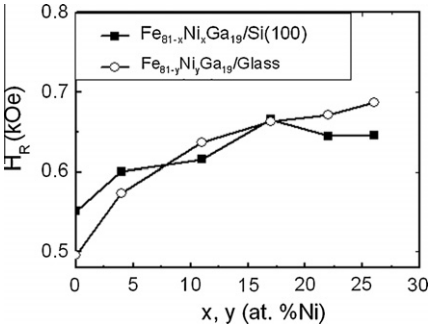

Fig. 3. The main resonance field (H_R), at f = 9.6 GHz, of the various FeNiGa films.

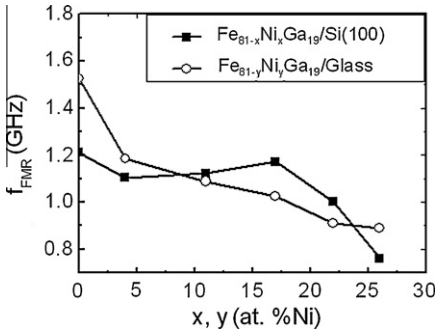

Fig. 4. Natural resonance frequency (f_{FMR}) of the FeNiGa films plotted vs. the Ni concentration (x or y).

Next, at low frequency, the definition of rotation permeability for an in-plane uniaxial film, such as any FeNiGa film in this study, is $\mu_r = 4\pi M_S/H_K$. Then, in Fig. 5, we can calculate μ_r of the FeNiGa films and plot it as a function of x or y. From this figure, we conclude that in general μ_r increases, as x or y increases. It is easy to understand this result; i.e., the Snoek's law, followed from the Landau–Lifshitz equation, can be written as [2,20],

$$(\mu_r - 1)f_{FMR}^2 = (\nu 4\pi M_s)^2 \tag{2}$$

In Eq. (2), $(\nu 4\pi M_S)$ of the FeNiGa films is almost independent of x or y; i.e. it decreases by only 10%, as x or y increases from 0 to 26 at.% Ni. However, based on Fig. 4 $(f_{FMR})^2$ decreases by 64%, as x or y increases similarly. Thus, from Eq. (2), there should be a trade-off between μ_r and f_{FMR} for both series of FeNiGa films.

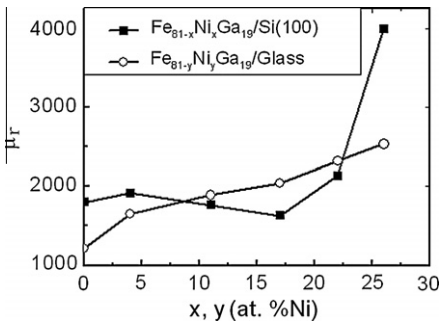

Fig. 5. Static rotational permeability (μ_r) increases, as x or y increases in the FeNiGa films.

For a ferromagnetic film, high speed magnetization switching means a low Gilbert damping parameter (α). From the Landau–Lifshitz–Gilbert (LLG) equation, the magnetic damping parameter (α) can be written as [20],

$$\alpha = \frac{\Delta f_{1/2}}{\nu 4\pi M_S} \tag{3}$$

where $\Delta f_{1/2}$ is the full width at half maximum for the absorption peak of μ_l at resonance. Eq. (3) is used in a shorted micro-strip transmission line perturbation experiment [20]. Alternatively, Eq. (3) can also be written as [18],

$$\alpha = \nu(\Delta H)_S/2f_{FMR}, \tag{4}$$

where $(\Delta H)_S$ is the *theoretical* full width at half maximum of the absorption peak around the main resonance field (H_R). Notice that the subscript "s" of ΔH in Eq. (4) means that this *theoretical* ΔH should be, in principle, symmetric with respect to the central peak, H_R. In the following, we shall give a reason for this argument. The LLG equation with Kittel mode can be expressed in the following form [18,19,21]:

$$\tan\phi = \frac{4\pi\lambda\mu_0}{\nu M_S}\frac{H}{H - H_R} \tag{5}$$

and

$$\mu_R \sim \chi' = \left(\frac{M_S}{\alpha H}\right)\sin\phi\cos\phi \tag{6a}$$

$$\mu_I \sim \chi'' = \left(\frac{M_S}{\alpha H}\right)\sin^2\phi \tag{6b}$$

where $\mu_o = 4\pi \times 10^{-7}$ H/m, ϕ is a finite azimuthal angle between the rotating field vector h_{rf} and the magnetization vector M_S, $\lambda \equiv (\alpha \nu M_S)/(4\pi\mu_o)$, and H is an in-plane field with EA//H. From Eq. (5), $\tan(\phi)$ reaches the maximum value, when $H = H_R$ or $\phi = 90°$. Similarly, from Eq. (6), the maximum χ'' also occurs at $\phi = 90°$. In other words, if Eqs. (5) and (6b) are combined, we obtain,

$$\mu_I \propto \sin^2\phi \propto \left[\frac{H^2}{H^2 + \left(\frac{1}{\alpha}\right)^2 (H - H_R)^2}\right]\left[\frac{M_S}{\alpha H}\right] \quad (7)$$

In Eq. (7), the Lorentzian part, $H^2/[H^2 + (1/\alpha)^2(H - H_R)^2]$, of μ_I must be symmetric with respect to (w.r.t.) H_R. However, the $(1/H)$ part of μ_I is not. Fortunately, when H is near H_R, the H dependence of μ_I is more characterized (or affected) by the Lorentzian part, if α is small, which is exactly the case for our films. Thus, we can still consider μ_I to be symmetric w.r.t. H_R. Further, since the FeNiGa films are metallic, due to the eddy current (or the surface impedance) effect, the power absorption of microwave at H_R should be expressed as [22],

$$\Delta P_{abs} = \left[(\mu_R^2 + \mu_I^2)^{1/2} + \mu_I\right]^{1/2}, \quad (8)$$

Thus, unlike a ferromagnetic insulator, there is an admixture of μ_R and μ_I in ΔP_{abs} for a ferromagnetic FeNiGa metal. From Eq. (6a), μ_R is mainly anti-symmetric w.r.t. H_R. But, $(\mu_R)^2$ in Eq. (8) is still symmetric w.r.t. H_R. As a result, no matter if the film is metallic or not, ΔP_{abs} is symmetric. Moreover, when H is near H_R, $(\mu_I)^2 >> (\mu_R)^2$, which leads to the result,

$$\Delta P_{abs} \cong \left[2\mu_I\right]^{1/2}, \quad (9)$$

from Eq. (8). Thus, we believe that in our case the *theoretical* ΔP_{abs} is symmetric w.r.t. H_R. Also, whether we used $\Delta P_{abs} \sim \mu_I$ or $\Delta P_{abs} \sim (2\mu_I)^{1/2}$, we should, in principle, always get the same $(\Delta H)_S$, and by definition the symmetric width $(\Delta H)_S \equiv 2\alpha H_R$, i.e., Eq. (4). However, in reality, as shown in Fig. 2, the *experimental* width $(\Delta H)_{exp}$ is not ideally symmetric. Hence, $(\Delta H)_{exp}$ is composed of two parts: $(\Delta H)_{exp} = (\Delta H)_S + (\Delta H)_A$, where $(\Delta H)_S$ and $(\Delta H)_A$ are the symmetric and asymmetric parts in $(\Delta H)_{exp}$. In general, three sources may contribute to $(\Delta H)_A$: one is from the structural inhomogeneity, and the other two are from the magnetic inhomogeneities [21]. As discussed previously, Table 1 shows that if $y = 22$ at.% Ni (range A), the films are structurally homogenous (i.e., containing only one A2 phase), and if $y = 0$–17, and 26 at.% Ni (range B), they are structurally inhomogenous (i.e., containing mixed phases). Thus, we expect that for the former film its $(\Delta H)_A$ is smaller, while for the latter films their $(\Delta H)_A$'s are larger. In agreement with the experimental data from FMR experiments (Table 1), for the film in range A, the degree of asymmetry of the linewidth, $(\Delta H)_A/(\Delta H)_{exp} = 0.9\%$, is smaller, while for those in range B, the degree of asymmetry, $(\Delta H)_A/(\Delta H)_{exp} = 3.6$–$19.7\%$, is larger in general. As to the magnetic inhomogeneity, one mechanism is due to the asymmetric distributions of the magnitude and/or angle dispersion of H_K. The other is associated with the local inhomogenous demagnetizing field (H_d) near edges of the film sample. Here, we are unable to assess how much the magnetic-inhomogeneity mechanisms would affect $(\Delta H)_A/(\Delta H)_{exp}$ quantitatively.

Fig. 6 shows that as y increases, α decreases from 0.060 to 0.013 for the FeNiGa films deposited on glass substrates, and as x increases, α first decreases from 0.052 to 0.020 and then increases from 0.020 to 0.050 for the FeNiGa films deposited on Si(100) substrates. All these Gilbert damping parameters were extracted, as described previously, from each FMR measurement made along the easy-axis. We like to emphasize that since all our films are poly-crystalline, α shown in Fig. 6 may or may not be from the minimum or maximum linewidth of each sample [23]. In addition, one may notice that there is discrepancy between α data of the x- and y-series films in the range $17 \leqslant x$ or $y \leqslant 26$ at.% Ni. In the following, we shall explain why the α data from the y-series ($Fe_{81-y}Ni_yGa_{19}$/glass) films should be more reliable. The p-doped Si(100) semiconductor substrate conducts with electrical resistivity (ρ), about 5–10 Ω cm. On the other hand, ρ is about 120–150 μΩ cm for FeNiGa films deposited on insulating glass. Further, the thickness ratio of t_{Si}/t_f is about 10^3. A simple calculation shows that the electrical resistance ratio, R_{Si}/R_f, for the x-series ($Fe_{81-x}Ni_xGa_{19}$/Si(100)) films is of the order of one. Thus, the current shunting effect must be significant in the case of FeNiGa films deposited on Si(100). As observed, the (apparent) ρ of the x-series films is in general smaller than the (real) ρ of the y-series films. In an FMR situation, the eddy current, i_{ac} induced by h_{rf}, must be flowing in the most conducting FeNiGa film at least. For the y-series film, because glass is an insulator, i_{ac} is mainly limited inside the film region. However, for the x-series films, due to the current shunting effect, i_{ac} will flow across the film/Si interface. Moreover, the spin injection across the interface indicates that the proximity region on the Si side, which is partially magnetized, will also absorb microwave, and make an extra contribution to the main FMR signal from the film. As a result, for the x-series ($Fe_{81-x}Ni_xGa_{19}$/Si(100)) films, there is an additional broadening of the FMR peak width due to the extraneous eddy-current effect near the film/Si interface [20]. Thus, in general α of the $Fe_{81-x}Ni_xGa_{19}$/Si(100) films, as shown in Fig. 6, should be less accurate (or meaningful) than that of the $Fe_{81-y}Ni_yGa_{19}$/glass films.

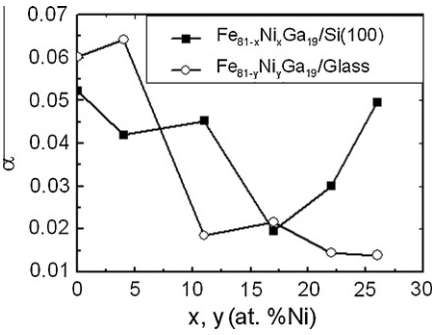

Fig. 6. Gilbert damping parameter (α) plotted as a function of the Ni concentration (x or y) for the FeNiGa films.

Fig. 7 shows λ_S of the x- and y-series FeNiGa films as a function of the Ni concentration (x or y). The general trend in Fig. 7 is that as x or y increases, λ_S increases, and λ_S reaches a local maximum when x and/or $y = 22$ at.% Ni. For $Fe_{59}Ni_{22}Ga_{19}$/Si(100), $\lambda_S = 19$ ppm, and for $Fe_{59}Ni_{22}Ga_{19}$/glass, $\lambda_S = 27$ ppm. Also, notice that the saturation field of these films is quite low, about 15 Oe only. Hence, its magnetostriction sensitivity, defined as $S_H \equiv (3/2)(\lambda_S/H_S)$, can be quite high, about 1.9–2.7 ppm/Oe, which is suitable for the low field and high frequency application.

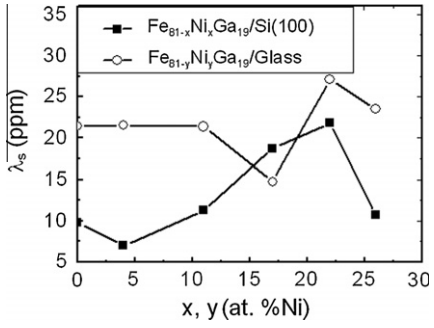

Fig. 7. Saturation magnetostriction (λ_S) reaches maximum, when x or $y = 22$ at.% Ni.

4. Conclusion

We have made two series of $Fe_{81-x}Ni_xGa_{19}$/Si(1 0 0) and $Fe_{81-y}Ni_yGa_{19}$/glass films, with $0 \leqslant x$ or $y \leqslant 26$ at.% Ni, at room temperature by the magnetron sputtering method. Magnetic hysteresis loop, magnetostriction, and FMR measurements were performed on these films. We observed that $(\Delta H)_{exp}$ of each film is in general asymmetric. Hence, $(\Delta H)_{exp}$ is composed of two parts: $(\Delta H)_{exp} = (\Delta H)_S + (\Delta H)_A$, where $(\Delta H)_S$ and $\Delta H)_A$ are the symmetric and asymmetric parts. We believe this asymmetry is related to the degrees of the structural and/or magnetic inhomogeneities in each film. As x or y increases from 0 to 26 at.% Ni, we found that (I) $4\pi M_S$ decreases only slightly, 16.6–15.0 KG, (II) H_C is small, 34.4–13.8 Oe; (III) λ_S first increases and reaches a local maximum at x or y = 22 at.% Ni; (IV) f_{FMR} tends to decrease, 1.6–0.8 GHz; (V) μ_R tends to increase, 1212–3993; and (VI) α decreases in general, 0.060–0.013.

Thus, from this study we conclude that among all the FeNiGa/glass films, the $Fe_{59}Ni_{22}Ga_{19}$/glass film should be the most suitable, due to its highest λ_S, S_H, ρ, (next to the highest) μ_r and the lowest H_S and (next to the lowest) α, for application in the magneto-electric microwave devices. However, $4\pi M_S$ and f_{FMR} of the $Fe_{59}Ni_{22}Ga_{19}$/glass film are relatively smaller.

Acknowledgement

This work is supported by a Grant No. NSC 100-2112-M-001-017-MY3, from the National Science Council.

Appendix A. Supplementary material

Supplementary data associated with this article can be found, in the online version, at http://dx.doi.org/10.1016/j.jallcom.2013.01.169.

References

[1] R. Boll, Soft Magnetic Materials, Heyden & Son, Hanau, 1979.
[2] S. Chikazumi, Physics of Magnetism, Krieger, New York, 1978.
[3] J. Lou, R.E. Insignares, Z. Cai, K.S. Ziemer, M. Liu, N.X. Sun, Appl. Phys. Lett. 91 (2007) 182504.
[4] A.E. Clark, J.B. Restorff, M. Wun-Fogle, T.A. Lograsso, D.L. Schlagel, IEEE Trans. Mang. 36 (2000) 3238.
[5] S.U. Jen, T.L. Tsai, J. Appl. Phys. 111 (2012) 07A939.
[6] A.E. Clark, M. Wun-Fogle, J.B. Restorff, T.A. Lograsso, Mater. Trans., JIM 43 (2002) 881.
[7] N. Srisukhumbowornchai, S. Guruswamy, J. Appl. Phys. 9 (2001) 5680.
[8] A. Butera, J. Gómez, J.L. Weston, J.A. Barnard, J. Appl. Phys. 98 (2005) 033901.
[9] Y. Gong, C. Jiang, H. Xu, Acta Metall. Sin. 42 (2006) 830.
[10] T. Kubota, A. Inoue, Mater. Trans. 45 (2004) 199.
[11] K. Fukamichi, T. Satoh, T. Masumoto, J. Magn. Magn. Mater. 31–34 (1983) 1589.
[12] J.B. Restorf, M. Wun-Fogle, A.E. Clark, T.A. Lograsso, A.R. Ross, D.L. Schlagel, J. Appl. Phys. 91 (2002) 8225.
[13] C. Bormio-Nunes, R. Sato Turtelli, H. Mueller, R. Grossinger, H. Sassik, M.A. Tirelli, J. Magn. Magn. Mater. 290–291 (2005) 820.
[14] C. Bormio-Nunes, R. Sato Turtelli, R. Grossinger, H. Muller, H. Sassik, J. Magn. Magn. Mater. 322 (2010) 1605.
[15] S. Middelhoek, Ferromagnetic Domains in Thin Ni–Fe Films, Drukkerij Wed. G. Van Soest N.V, Amsterdam, 1961.
[16] S.U. Jen, C.C. Lin, Thin Solid Films 471 (2005) 218.
[17] S.U. Jen, T.Y. Chou, C.K. Lo, Nanoscale Res. Lett. 6 (2011) 468.
[18] A.H. Morrish, The Physical Principles of Magnetism, John Wiley & Sons, New York, 1965.
[19] B.D. Cullity, C.D. Graham, Introduction to Magnetic Materials, John Wiley & Sons, New York, 2009.
[20] J.S. Liao, Z.K. Feng, J. Qiu, Y.Q. Tong, Acta Metall. Sin. 21 (2008) 419.
[21] S.V. Vonsovskii, Ferromagnetic Resonance, Pergamon Press, Oxford, 1966.
[22] N. Bloembergen, Phys. Rev. 78 (1950) 572.
[23] A. Butera, J.L. Weston, J.A. Barnard, J. magn. Magn. Mater. 284 (2004) 17.